

## Effective adsorption of Cr (VI) ions onto titanium dioxide immobilized high strength polyacrylamide hydrogels

Emre Tekay<sup>1</sup>, Demet Aydınoglu<sup>2</sup>, Ayşe N. Ökte<sup>3</sup>, Sinan Şen<sup>1\*</sup>

<sup>1</sup>Department of Polymer Engineering, Yalova University, Yalova, 77100, Turkey

<sup>2</sup>Department of Food Process Technologies, Yalova University, Yalova, 77500, Turkey

<sup>3</sup>Department of Chemistry, Boğaziçi University, İstanbul, 34342, Turkey

Corresponding author: Sinan Şen

---

**Abstract:** The “2-in-1” type polyacrylamide (PAAm) composite hydrogel adsorbents were prepared by in-situ polymerization reaction of acrylamide (AAm) monomer in presence of nano-sized TiO<sub>2</sub> particles together with a chemical crosslinker. The TiO<sub>2</sub> anatase nano-particles were synthesized by an acid-catalyzed sol-gel method from an alkoxide precursor. The morphological characterization of the hydrogels was done with SEM analyses. Their Cr(VI) ion adsorption capacities and wet strength properties were investigated via UV-Vis spectrophotometer and uniaxial compression tests, respectively. All the composite hydrogels showed higher swelling and adsorption performances than pure PAAm hydrogel. The neat hydrogel was found to adsorb 2.26 mg Cr(VI) per g hydrogel. On the other hand, the composite hydrogel having 0.1 wt% TiO<sub>2</sub> was found to have the highest Cr(VI) adsorption which is 8.13 mg Cr(VI) per g hydrogel and about 260 % higher than that of neat PAAm hydrogel. This result is quite remarkable since the pure TiO<sub>2</sub> synthesized adsorbed only 1.78 mg Cr(VI) per g nano-particle. The compression modulus, strength and toughness of the hydrogel in its wet form were found to be increased by about 80 %, 200 % and 120 %, respectively even at 0.1 wt% loading of the TiO<sub>2</sub>, compared to neat hydrogel

**Keywords:** Titanium dioxide nanoparticles, composite hydrogel, adsorption, isotherm, wet strength

---

### I. INTRODUCTION

The water pollution has been an important issue of recent years due to its toxic pollutants like heavy metals, leading to an environmental damage. Industrial effluent generally includes poisonous heavy metal ions like Cr (VI), Pb (II), Ni (II), Cd (II) and Zn (II) [1]. As a strong oxidant, hexavalent chromium ion Cr (VI) in contaminated industrial water streams is known to be highly dangerous for human health because of its carcinogenic effect and high permeability into biological membrane [2]. Much has been done for the removal of Cr (VI) ions (Cr<sub>2</sub>O<sub>7</sub><sup>2-</sup>, HCrO<sub>4</sub><sup>-</sup>, CrO<sub>4</sub><sup>2-</sup> and HCrO<sub>7</sub><sup>-</sup>; depending on pH and concentration) from wastewater by using different kinds of adsorbents like bentonite [3], algae [4], composite hydrogels [5-6] and nanosized metal oxides (NMOs) [7].

Polyacrylamide (PAAm) based hydrogels have been widely used as adsorbents in many sorbent applications. However, like other hydrogels, their porous structures exhibit poor mechanical properties in their wet states, limiting their use in adsorption and other applications. This disadvantage has been overcome by preparing interpenetrating polymer networks [8-9] and composite hydrogels with organic nanoparticle [10] and inorganic nanoparticle [5] addition.

Among many adsorbents, nanosized metal oxides (NMOs) such as magnesium oxides, aluminum oxides, titanium oxides and ferric oxides have been widely studied for the removal of heavy metals since they present high surface area and affinity for the adsorption [7]. Maghemite (Fe<sub>2</sub>O<sub>3</sub>) as a ferric oxide, cerium oxide (CeO<sub>2</sub>) nanoparticles and iron oxyhydroxide [7, 11] were reported to have been used as adsorbents for the Cr (VI) ions. Unlike these nanosized metal adsorbents, the use of TiO<sub>2</sub> (anatase) particles for chromium adsorption is quite limited. TiO<sub>2</sub> is a chemically stable and low-cost material as well as an effective photocatalyst for degradation of organic pollutants [12]. TiO<sub>2</sub> as one of nontoxic materials, has surface hydroxyl groups (OH) interacting with heavy metal ions in wastewater resulting in their adsorption. Depending on the surface acidity, the hydroxyl groups are found in protonated (TiOH<sub>2</sub><sup>+</sup>), neutral (TiOH) and ionized (TiO<sup>-</sup>) forms. In neutral pH conditions (pH 5.5-6.0), TiOH and TiOH<sub>2</sub><sup>+</sup> are both present on the adsorbent surface [13]. Weng et al [13] studied the adsorption of Cr (VI) ion by using TiO<sub>2</sub> anatase particle as received-form, having an average size of 30 nm. The maximum adsorption (142 µmol/g) together with Langmuir model fitting was achieved at pH 5.0 for 1 ppm of Cr(VI) solution in presence of sodium perchlorate electrolyte.

On the other hand, agglomeration/aggregation of fine NMOs particles in a suspension and its separation/recovery difficulties limit their use in their pure forms. For an effective adsorption, hybrid adsorbents of NMOs (host supported NMOs) have been prepared by using different types of supports; natural supports, polymeric porous hosts and metallic oxides [7]. Iron oxide immobilized graphene nanosheets [14] and

manganese oxide modified sand [15] are the two examples of the hybrid adsorbents used for Cr (VI) adsorption in the literature. TiO<sub>2</sub> particles have also been immobilized on some adsorbent/support systems such as layered double hydroxides [16], zeolite [17], soda lime glass [18], and clays [19-20]. However, all these abovementioned supported-TiO<sub>2</sub> hybrid adsorbents were used to investigate their photocatalytic activities for only organic pollutants like methyl orange and not used for heavy metal removal process. Therefore, a systematic study on adsorption performance of supported-TiO<sub>2</sub> particles for heavy metals seems to be needed.

This paper reports the use of TiO<sub>2</sub> reinforced hydrogel adsorber for Cr (VI) ion from aqueous solution. By this way, we aimed to obtain a “2-in-1” type adsorber system with high strength and toughness. PAAm hydrogel having high swelling and low adsorption was combined with TiO<sub>2</sub> nanoparticle in one material. For this purpose, nano-sized TiO<sub>2</sub> particle was synthesized from an acid-catalyzed sol-gel method from an alkoxide precursor, as described in the study of Ökte et al. [21]. Then, the composite hydrogels were synthesized by in-situ polymerization of acrylamide monomer in presence of the TiO<sub>2</sub> particle. The PAAm hydrogel is known easily-prepared material, also providing additional adsorption properties. The immobilization of TiO<sub>2</sub> in/on the hydrogel support may cause high amount of surface area/hydroxyl groups to interact with chromate ions through ionic and/or ion-dipole interactions. Therefore, the synthesized pure TiO<sub>2</sub> particle in the hydrogel supported form is expected to adsorb much more chromate ions from the aqueous solution as compared to abovementioned studies having only TiO<sub>2</sub> as adsorbent [12-13]. It is also believed that use of TiO<sub>2</sub> within the PAAm hydrogel system will provide its easy removal from the aqueous medium as a bulk after the adsorption test. This will eliminate repeated centrifuging process of the aqueous solution, generally done to get adsorbent free solution before testing [22-23]. This will be an important practical advantage of the proposed “2-in-1” adsorbent system. Besides, TiO<sub>2</sub> in this study is also thought to increase the strength of weak porous hydrogel system by reinforcing it, which was expected as another advantage especially for swollen state of the adsorber. Differences in water absorption, metal adsorption, morphologies and wet strength of the resultant composite hydrogels were discussed as a function of degree of TiO<sub>2</sub> loading.

## II. EXPERIMENTAL

### 2.1. Materials

Acrylamide (AAm), the initiator, ammonium persulfate (APS) the activator, sodium metabisulfite (SMBS) and acetic acid (96 %) were used as provided by Merck (Darmstadt, Germany). The cross-linker, *N,N* methylene bis-acrylamide (BAAm), potassium dichromate (K<sub>2</sub>Cr<sub>2</sub>O<sub>7</sub>), Diphenyl carbazide and titanium tetraisopropoxide (98 %) were obtained from Aldrich Chemicals (Milwaukee, WI).

### 2.2. Synthesis of TiO<sub>2</sub> particles

TiO<sub>2</sub> was prepared by means of an acid-catalyzed sol-gel method from an alkoxide precursor [21, 24-25]. The typical procedure as follows: 20 mL of titanium tetraisopropoxide was added gradually to 80 wt% acetic acid solution at 50 °C to produce a transparent sol. At the end of 2 h continuous stirring, the sol was dried at 100 °C for 12 h. Then, a suspension was prepared with deionized water and agitated by magnetic stirrer for 12 h at room temperature. After several washings and centrifugations, the resulting particles were dried at 100 °C for 12 h and calcined at 200 °C and 500 °C for 5 h, and named as TiO<sub>2</sub> (100 °C), TiO<sub>2</sub> (200 °C) and TiO<sub>2</sub> (500 °C).

### 2.3. Preparation of PAAm composite hydrogels

In the synthesis of composite hydrogels, the anatase-rich TiO<sub>2</sub> nanoparticle was used as co-adsorber/reinforcer [26]. PAAm composite hydrogels were prepared with a similar procedure as described in our recent study [5]. AAm was polymerized by in situ technique in presence of the TiO<sub>2</sub> and the organic cross-linker, BAAm. The reaction solution consisting of deionized water (10 mL), AAm (0.572 g) and various amounts of TiO<sub>2</sub> (0.1 %, 0.5 % and 1 % by weight of monomer) was prepared. Then the cross-linker, BAAm (1 mol% with respect to monomer) was added to this solution. After the monomer and the cross-linker were dissolved, the redox initiator couple, SMBS (0.1 mol%, based on the monomer) and APS (0.3 mol%, based on the monomer) were added to this solution with stirring. The hydrogels were synthesized in airtight glass tubes. Then, the polymerization was conducted in a water bath at 35 °C for 48 h. The hydrogels having 2 wt% and 3 wt% of TiO<sub>2</sub> were also prepared but large aggregates occurred in the structure, resulting in phase separation. So they were not used for the subsequent studies.

The resultant composite hydrogels are referred as H-XTiO<sub>2</sub>, where X represents the loading percent of TiO<sub>2</sub>. The hydrogels were cut into disc-like pieces for the characterization studies.

## 2.4. Characterization

The TiO<sub>2</sub> particle was analyzed by using X-ray diffraction (XRD) using a Rigaku D/Max 2200 Ultimat diffractometer (Rigaku, Tokyo, Japan) with CuK $\alpha$  radiation ( $\lambda=15.4$  nm), operating at 40 kV and 40 mA with 2°/min scanning rate. Morphological characterization was done by SEM analyses using ESEM-FEG/EDAX Philips XL-30 (Philips, Eindhoven, The Netherlands) in combination with energy dispersive X-ray analysis. Before the SEM observation, the samples were coated with platinum using a sputter coater.

Swelling experiments were conducted by gravimetric measurements in deionized water at room temperature. The freeze-dried polymeric samples were put into deionized water and taken out at regular intervals to measure change in weight. Water uptake with respect to time was recorded until the swelling equilibrium was reached. The measurements were carried out at 25 °C in a water bath. The equilibrium swelling as percentage was calculated as follows:

$$S\% = \frac{m_s - m_0}{m_0} * 100 \quad (1)$$

where  $m_s$  is the mass of the swollen gel and  $m_0$  is the mass of the dry gel.

The compression test was performed by doing a uniaxial compression experiment for the swollen hydrogels at room temperature and at a compression rate of 2 mm min<sup>-1</sup>. The measurements were conducted with a Zwick/Roell Z1.0 Universal Testing Machine (Zwick GmbH & Co.KG, Germany) equipped with a 50 N load cell until the samples break. Adsorption behaviors of the hydrogels and the synthesized TiO<sub>2</sub> were investigated by UV/VIS measurements. The dry hydrogels were put into 100 mL of solutions of different Cr (VI) concentrations (50, 100, 150 and 200 ppm), separately. The UV analyses of the solutions at a pH of 5.5-6.0 were carried out by using a UV-VIS spectrophotometer (Optizen Pop Spectrophotometer, Daejon, South Korea) and Diphenyl carbazide “3500-Cr” technique at 540 nm [27]. The amount of adsorbed Cr (VI) as a function of time was found for the hydrogels and the TiO<sub>2</sub> by the metal solution with concentration of 50 ppm whereas adsorption isotherms were obtained from abovementioned four different concentrations of the metal solution. Then, the metal adsorption ( $q_e$ ) as amount of Cr (VI) was measured with the following equation:

$$q_e(\text{mg Cr(VI)/g hydrogel}) = \frac{\sum (C_i - C_f) \times V}{W} \quad (2)$$

where  $C_i$  and  $C_f$  are the initial and final concentrations of metal ions in the solution (mg L<sup>-1</sup>) at each time intervals,  $V$  is the volume of the metal ion solution (L),  $W$  is the weight of the dry hydrogel used in the experiment (g) [6].

## III. RESULTS AND DISCUSSION

### 3.1. Characterization of TiO<sub>2</sub>

Fig. 1 illustrates XRD spectrums of TiO<sub>2</sub> (100 °C), TiO<sub>2</sub> (200 °C) and TiO<sub>2</sub> (500 °C). The intense signal was noticed at 25.3° (2 $\theta$ ) due to  $d_{101}$  plane of anatase. The other characteristic anatase diffractions of  $d_{103}$ ,  $d_{004}$ ,  $d_{112}$ ,  $d_{200}$ ,  $d_{105}$  and  $d_{211}$  appeared at 37, 37.8, 38.6, 48, 54, and 55° (2 $\theta$ ), respectively. The crystalline sizes of TiO<sub>2</sub> nanoparticles were calculated from the  $d_{101}$  peak broadening by employing the Scherrer’s equation as 12.29 nm for TiO<sub>2</sub> (100 °C), 12.67 nm for TiO<sub>2</sub> (200 °C) and 17.83 nm for TiO<sub>2</sub> (500 °C). Heat treatment induced sharper and narrower X-ray peaks was also noticed by Chen et al. [28]. This enhances the crystallinity of titania nanoparticles.

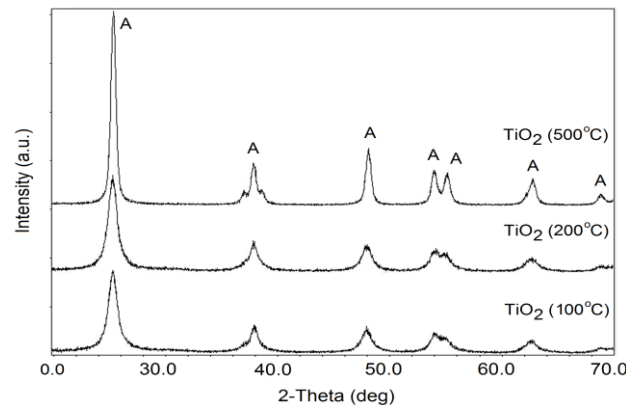


**Fig. 1** XRD patterns of TiO<sub>2</sub> (100°C), TiO<sub>2</sub> (200°C) and TiO<sub>2</sub> (500°C) nanoparticles (A: Anatase).

### 3.2. Morphological analyses of hydrogels

All the composite hydrogels were synthesized by using  $\text{TiO}_2$  (500 °C) nanoparticle since it has much higher amount of anatase crystalline form (Fig. 1) providing large surface area [26]. Fig. 2 shows SEM images of inner surfaces of neat PAAm and  $\text{TiO}_2$  loaded hydrogels. It is seen from the figure that neat hydrogel includes pores with sizes of *ca.* 230 micron. The  $\text{TiO}_2$  loaded hydrogels, H-0.1Ti and H-0.5Ti resulted in pores with almost the same size as neat one. For the H-1.0Ti hydrogel, pore size was found to be heterogeneous and decrease to *ca.* 125 micron with few larges ones. The formation of such smaller pores may be resulted from additional physical crosslinks taking place between polymer chains' polar groups and  $\text{TiO}_2$  surfaces.

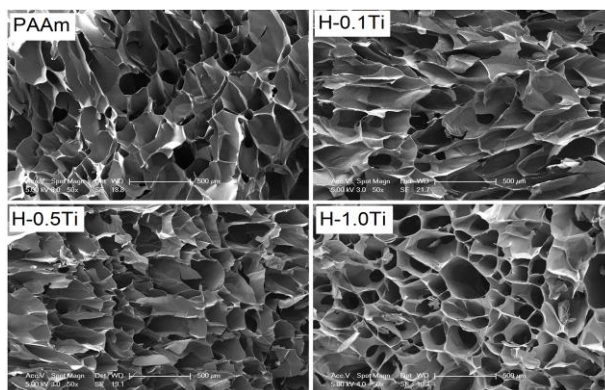


**Fig. 2** SEM images of inner surfaces of neat and composite hydrogels.

Fig. 3 exhibits high magnification SEM images of H-0.1Ti, H-0.5Ti and H-1.0Ti hydrogels' cell walls and their X-ray scans for elemental Ti of the same areas. The agglomerates seen in the images of H-0.5Ti and H-1.0Ti hydrogels correspond to  $\text{TiO}_2$  particles immobilized on the hydrogels. The corresponding mapping images of their surfaces were found to have large aggregated particles about 2 micron and 6 micron in size, respectively. It may be caused by interactions of  $\text{TiO}_2$  particles with each other at higher loading. On the other hand, H-0.1Ti hydrogel shows no agglomeration in its Ti mapping image suggesting that  $\text{TiO}_2$  particles were homogeneously dispersed in the matrix at its lower degree of loading. The fine dispersion of  $\text{TiO}_2$  particles in the hydrogel may also result in their size to be too small to be observed under the SEM resolution.

### 3.3. Swelling behavior of hydrogels

Fig. 4 shows the swelling test results of neat hydrogel and composite hydrogels. It can be seen from the figure that equilibrium swelling for all the hydrogels does not seem to change so much. Neat PAAm hydrogel has an equilibrium swelling of 2087 %. The swelling increases with increase in  $\text{TiO}_2$  loading and the maximum swelling (2515 %) was achieved via H-1.0Ti. The higher water-uptake in these composite hydrogels may be attributed to hydrophilic surface of  $\text{TiO}_2$ . On the other hand, all the composite hydrogels were found to have higher swelling rates especially up to 5000 minutes in comparison with pure PAAm hydrogel. A 30 % and 15 % increase in the swelling rate was achieved for H-0.5Ti and H-1TiM hydrogels, respectively.

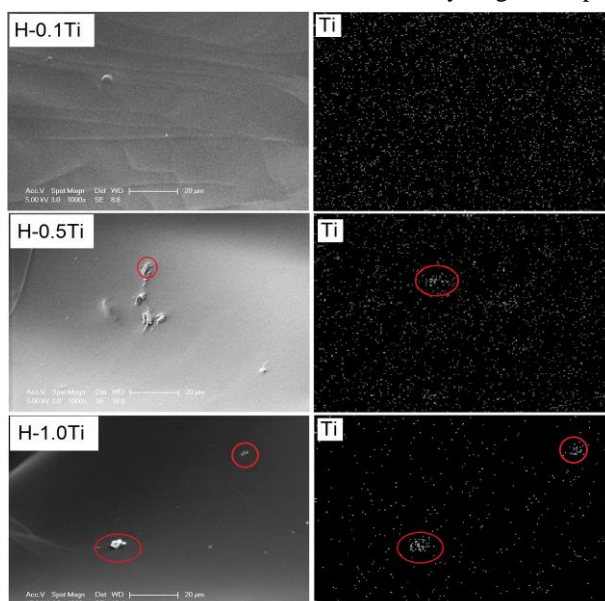


**Fig. 3** High magnification SEM images and corresponding X-ray scans for titanium of composite hydrogels.

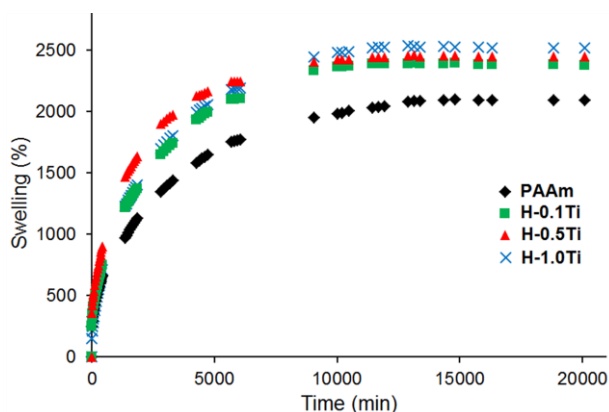


Fig. 4 Percentage swelling of neat PAAm hydrogel and composite hydrogels having TiO<sub>2</sub>.

### 3.4. Metal Adsorption Behavior of Hydrogels

The uptake of Cr (VI) ions by the hydrogels and the TiO<sub>2</sub> synthesized from an acid-catalyzed sol-gel method was detected with the help of UV/Vis analyses. The resultant adsorption data as a function of time were plotted in Fig. 5. As it was mentioned before, the surface hydroxyl groups of TiO<sub>2</sub> particles are found in both TiOH and TiOH<sub>2</sub><sup>+</sup> forms under the adsorption test conditions (pH: 5.5-6.0) [13]. The maximum Cr (VI) ion adsorption of neat hydrogel and the TiO<sub>2</sub> were found to be 2.26 mg per g of the hydrogel (Fig. 5a) and 1.78 mg per g of the TiO<sub>2</sub> (Fig. 5b), respectively, in the 50 ppm solution. On the other hand, it increased to 8.13, 4.72 and 2.35 mg per g for H-0.1Ti, H-0.5Ti and H-1.0 hydrogels, respectively. The increased adsorption data obtained by composite hydrogels can be ascribed to interaction of neutral and positively charged surfaces of TiO<sub>2</sub> and chromate ions through dipole-dipole and ionic interactions. The H-0.1Ti as the most efficient composite hydrogel exhibited 260 % higher adsorption capacity than the pure PAAm hydrogel and was found to adsorb about 800 % chromate ions with respect to the weight of its TiO<sub>2</sub> content in the 50 ppm solution. Moreover, when the difficulty in removal process of powder form of TiO<sub>2</sub> adsorbent from the solution is considered, “hydrogel supported-TiO<sub>2</sub> (“2-in-1” type) adsorber” system seems to be more advantageous. On the other hand, the lower adsorption capacities at high degree of loadings (0.5 % and 1.0 % TiO<sub>2</sub>) are in good agreement with their corresponding SEM images showing the presence of much smaller pores in different sizes (Fig. 2) and inhomogeneous distribution of TiO<sub>2</sub> particles (Fig. 3).

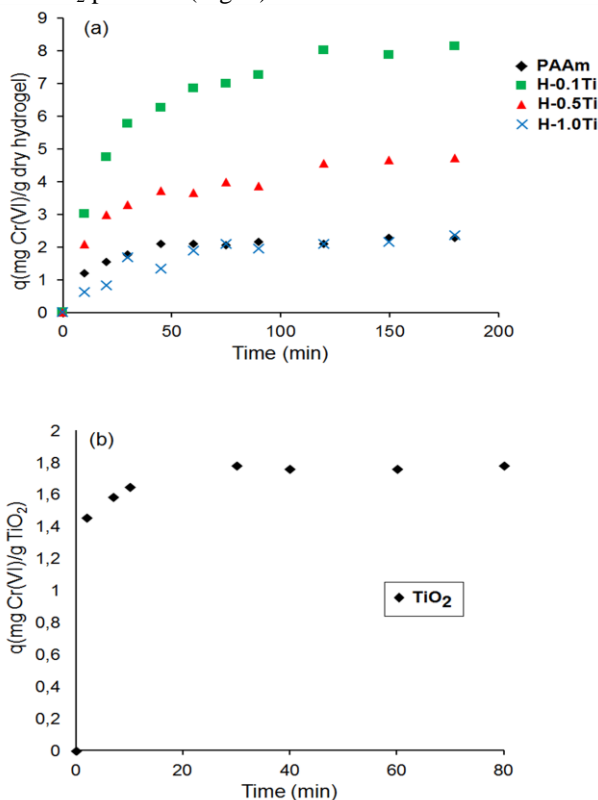


Fig. 5 Metal adsorption capacities of (a) PAAm hydrogels and (b) the synthesized TiO<sub>2</sub>.

Freundlich adsorption model used for heterogeneous surfaces [29] was applied for the composite hydrogels to find their adsorption isotherm data.

Different concentrations (50-200 mg L<sup>-1</sup>) of chromium (VI) solutions were tested and adsorption capacity  $q_e$  (mg g<sup>-1</sup>) and equilibrium Cr (VI) concentration,  $C_e$  (mg L<sup>-1</sup>) were calculated. Fig. 6 shows adsorption capacity  $q_e$  (mg g<sup>-1</sup>) as a function of initial metal ion concentration  $C_o$  (mg L<sup>-1</sup>). It is clear from the figure that all the composite hydrogels showed an increased metal adsorption value with increase in initial metal ion concentration. Among all the hydrogels, the H-0.1Ti showed much higher adsorption capacity for each metal ion concentrations. The highest adsorption value (17.54 mg g<sup>-1</sup>) was obtained for H-0.1Ti hydrogel at the highest concentration (200 mg L<sup>-1</sup>). The equilibrium metal ion concentration ( $C_e$ , mg L<sup>-1</sup>) was also determined and the log  $q_e$ -log  $C_e$  curves were shown in Fig. 7.

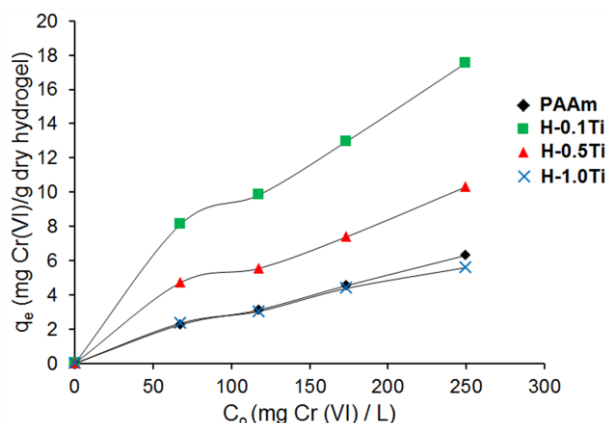


Fig. 6 Effect of initial metal concentration on metal adsorption by neat PAAm hydrogel and composite hydrogels.

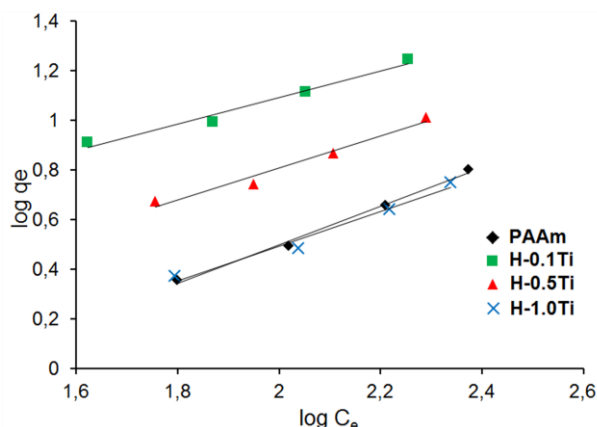


Fig. 7 Linearized Freundlich isotherms of metal adsorption capacities of the hydrogels.

The adsorption constants; adsorption capacity ( $k$ ), adsorption intensity ( $n$ ) and correlation coefficient ( $r^2$ ) were computed from the  $q_e$  and  $C_e$  values and the results were given in Table 1. It is clearly observed from the table that all the composite hydrogels showed higher  $k$  values than neat hydrogel which is in good agreement with their higher swelling values (Fig. 4). The maximum adsorption capacity ( $k$ ) value was found to be 1.05 for H-0.1Ti hydrogel as the most effective adsorbent for Cr (VI) based on the Freundlich adsorption model. This result is highly consistent with its metal adsorption behavior as a function of time (Fig. 5a). On the other hand, the lowest  $k$  value of H-3.0Ti hydrogel can be attributed to poor dispersion of TiO<sub>2</sub> particles at high loading (Fig. 3) which results in relatively lower surface area for the interaction of chromate ions. Nevertheless, H-1.0Ti hydrogel has higher adsorption value than neat hydrogel.

Table 1. Freundlich Constants of Cr (VI) Adsorption by Hydrogels

Hydrogel	$k$	$1/n$	$r^2$
PAAm	0.08±0.002	0.77	0.994
H-0.1Ti	1.05±0.054	0.53	0.975
H-0.5Ti	0.32±0.019	0.64	0.970
H-1.0Ti	0.12±0.007	0.69	0.974

From the adsorption test results, it can be concluded that if optimum compositions are used, TiO<sub>2</sub> containing “2-in-1” type composite hydrogel can be tuned to be the best adsorbent system for removal of chromate ions. The composite hydrogel serving as the effective adsorber can be obtained due to additional receptor groups (OH and OH<sub>2</sub><sup>+</sup>) of TiO<sub>2</sub> particles which are homogeneously dispersed in the matrix at optimum loading degree.

### 3.5. Mechanical properties of hydrogels

Mechanical properties of the hydrogels at their maximum swollen states were investigated by a uniaxial compression test and the stress-deformation curves were given in Fig. 8. The mechanical test data were tabulated in Table 2. In order to follow the moduli of the hydrogels, initial parts of the curves were also added in an inset figure in Fig. 8. The inset figure in Fig. 8 shows an expansion of deformation percentage range of 0-5 %, showing compression modulus change of the samples. The pure PAAm hydrogel exhibited a compression modulus of 3.91 kPa. This value was found to be increased by addition of the TiO<sub>2</sub> nanoparticles in all the composite hydrogels. The reason for the higher moduli values may be attributed to physical interactions between the surface hydroxyl groups (TiOH, TiOH<sub>2</sub><sup>+</sup>) of the TiO<sub>2</sub> and the polymer matrix chains leading to restriction of polymer chains. The highest compression modulus was achieved via H-0.1Ti hydrogel and it is almost 80 % higher than that of neat hydrogel. This can be most probably due to fine and homogeneously dispersed TiO<sub>2</sub> particles (Fig. 3) that provide the largest surface area for interacting with polymer matrix. Then, the modulus exhibited a small decrease with increase in the amount of the TiO<sub>2</sub> above 0.1 %, but it is still much higher than that of neat hydrogel.

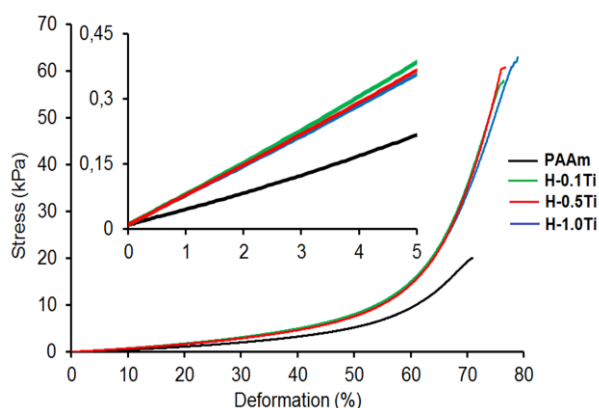


**Fig. 8** Compression stress-deformation curves for neat PAAm and composite hydrogels.

Moreover, all the composite hydrogels showed increased compression strength and toughness (work to break) values as compared to neat PAAm. This enhancement can be ascribed to abovementioned non-covalent interactions between the polymer matrix and the nanoparticles. These reversible physical crosslinks are also known to impart more viscous character and good distribution of the stress or energy in the main crosslink system [30-31]. The highest compression strength and toughness were obtained with H-1.0Ti composite hydrogel and are 218 % and 130 % higher than those of pure PAAm hydrogel, respectively (Table 2). The high performance of H-1.0Ti composite may also be assigned to its special morphological structure having lots of much smaller pores as compared to other composite hydrogels (Fig. 2d). The presence of these small-sized pores resulting from more physical crosslinks at the highest loading of TiO<sub>2</sub> may provide more effective dispersion of the compressive stress through the network system [32].

Finally, it can be safely stated that incorporation of the TiO<sub>2</sub> particle into PAAm hydrogel system enhances both adsorption and mechanical properties by providing additional functional groups and reinforcing it through the aforementioned interactions, respectively. The improvement of both the modulus and the toughness by even 0.1 wt% of TiO<sub>2</sub> particles can be ascribed to its fine and homogeneous distribution in the polymer matrix as reported in the literature [33].

**Table 2.** Mechanical Properties of The Hydrogels

Hydrogel	Compression Modulus (kPa)	Compression Strength (kPa)	Toughness (Nmm)
PAAm	3.91	19.62	5.18
H-0.1Ti	7.17	57.04	32.95
H-0.5Ti	6.95	59.93	32.00
H-1.0Ti	6.71	62.50	35.14

#### IV. CONCLUSION

The TiO<sub>2</sub> immobilized high strength and tough “2-in-1 type polyacrylamide (PAAm) composite hydrogels were synthesized. The crosslinking polymerization reaction of acrylamide was done with *N,N* methylene bis-acrylamide (BAAm) crosslinker in presence of the synthesized TiO<sub>2</sub>. All the composite hydrogels showed higher swelling and mechanical properties as compared to neat PAAm hydrogel. The mechanical test results showed that the compression modulus, strength and toughness increased with composite hydrogels. This was attributed to physical interactions between the surface functional groups of TiO<sub>2</sub> and the polar polymer molecules. Also, all the composite hydrogels served as effective adsorbers since they present both porous and polar matrix structure and additional receptors (OH and OH<sub>2</sub><sup>+</sup>) of TiO<sub>2</sub> in the same material. The composite hydrogel containing 0.1 wt% titanium dioxide with respect to monomer removed 8.13 mg Cr(VI) per g hydrogel and exhibited ca 260 % higher adsorption capacity than neat polyacrylamide hydrogel. On the other hand, pure TiO<sub>2</sub> and neat hydrogel adsorbed only 1.78 mg and 2.26 mg Cr(VI) per g, respectively. The highest adsorption performance of H-0.1Ti was achieved via TiO<sub>2</sub> particles which are homogeneously dispersed in the matrix at its low degree of loading. Also, according to Freundlich adsorption isotherms that H-0.1Ti hydrogel was found to have the maximum adsorption capacity value (k) as 1.05. When these enhanced adsorption capacities are considered, it can be concluded that “2-in-1” type novel hybrid composite adsorbers with high strength and toughness can be prepared with TiO<sub>2</sub> metal oxide immobilized / reinforced hydrogels at optimum composition.

#### ACKNOWLEDGEMENTS

This work was supported by Scientific Research Projects Coordination Departments of Yalova University (project no. 2013/YL/018) and Boğaziçi University (project no.11B05P4/6322).

#### REFERENCES

- [1] M. Bilgin, and S. Tulun, Removal of Heavy Metals (Cu, Cd and Zn) from contaminated soils using EDTA and FeCl<sub>3</sub>, *Global NEST Journal*, 18, 2016, 98-107.
- [2] W. Jinhua, Z. Xiang, Z. Bing, Z. Yafei, Z. Rui, L. Jindun and C. Rongfeng, Rapid adsorption of Cr (VI) on modified halloysite nanotubes, *Desalination*, 259, 2010, 22-28.
- [3] O. Maryuk, S. Pikus, E. Olszewska, M. Majdan, H. Skrzypek and E. Zieba, Benzyltrimethyloctadecylammonium bentonite in chromates adsorption, *Materials Letters*, 59, 2005, 2015-2017.
- [4] V.K. Gupta and A. Rastogi, Biosorption of hexavalent chromium by raw and acid treated green alga *Oedogonium hatei* from aqueous solutions, *Journal of Hazardous Materials*, 163, 2009, 396-402.
- [5] D. Aydınoglu, Ö. Akgül, V. Bayram and S. Şen, Polymer nanocomposite hydrogels with improved metal adsorption capacity and swelling behavior: influence of spirulina immobilization onto montmorillonite clay, *Polymer-Plastics Technology and Engineering*, 53, 2014, 1706-1722.
- [6] E. Tekay, S. Şen, D. Aydınoglu and N. Nugay, Biosorbent immobilized nanotube reinforced hydrogel carriers for heavy metal removal processes, *E-Polymers*, 16, 2016, 15-24.
- [7] M. Hua, S. Zhang, B. Pan, W. Zhang, L. Lv and Q. Zhang, Heavy metal removal from water/wastewater by nanosized metal oxides: A review, *Journal of Hazardous Materials*, 211-212, 2012, 317-331.
- [8] B. Li, Y. Jiang, Y. Liu, Y. Wu, H. Ren, B. Zhu and M. Zhu, Preparation and characterization of inorganic/ organic crosslinking poly(N-isopropylacrylamide)/ poly(acrylamide) interpenetrating network hydrogels, *Acta Polymerica Sinica*, 5, 2009, 419-424.
- [9] J. Lin, S. Xu, X. Shi, S. Feng and J. Wang, Synthesis and properties of a novel double network nanocomposite hydrogel, *Polymers for Advanced Technologies*, 20, 2009, 645-649.
- [10] Y.T. Wu, Z. Zou and Q.Q. Fan, Facile in-situ fabrication of novel organic nanoparticle hydrogels with excellent mechanical properties, *Journal of Materials Chemistry*, 19, 2009, 7340-7346.
- [11] J.M. Zachara, D.C. Girvin, R.L. Schmidt and C.T. Resch, Chromate adsorption on amorphous iron oxyhydroxide in presence of major groundwater ions, *Environmental Science and Technology*, 21, 1987, 589-594.
- [12] S. Asuha, X.G. Zhou and S. Zhao, Adsorption of methyl orange and Cr(VI) on mesoporous TiO<sub>2</sub> prepared by hydrothermal method, *Journal of Hazardous Materials*, 181, 2010, 204-210.
- [13] C.H. Weng, J.H. Wang and C.P. Huang, Adsorption of Cr(VI) onto TiO<sub>2</sub> from dilute aqueous solutions, *Water Science and Technology*, 35, 1997, 55-62.
- [14] H.Y. Koo, H.J. Lee, H.A. Go, Y.B. Lee, T.S. Bae, J.K. Kim and W.S. Choi, Graphene based multifunctional iron oxide nanosheets with tunable properties, *Chemistry - A European Journal*, 17, 2011, 1214-1219.
- [15] S.M. Lee, W.G. Kim, C. Laldawngliana and D. Tiwari, Removal behavior of surface modified sand for Cd(II) and Cr(VI) from aqueous solutions, *Journal of Chemical and Engineering Data*, 55, 2010, 3089-3094.
- [16] S. Pausova, J. Krysa, J. Jirkovsky, G. Mailhot and V. Prevot, Photocatalytic behavior of nanosized TiO<sub>2</sub> immobilized on layered double hydroxides by delamination/restacking process, *Environmental Science and Pollution Research International*, 19, 2012, 3709-3718.
- [17] A.N. Ökte and Ö. Yılmaz, Characteristics of lanthanum loaded TiO<sub>2</sub>-ZSM-5 photocatalysts: Decolorization and degradation processes of methyl orange, *Applied Catalysis A: General*, 354, 2009, 132-142.
- [18] P. Novotna, J. Krysa, J. Maixner, P. Kluson and P. Novak, Photocatalytic activity of sol-gel TiO<sub>2</sub> thin films deposited on soda lime glass and soda lime glass precoated with a SiO<sub>2</sub> layer, *Surface and Coatings Technology*, 204, 2010, 2570-2575.
- [19] R. Djellabi, M.F. Ghorab, G. Cerrato, S. Morandi, S. Gatto, V. Oldani, A. Di Michele and C.L. Bianchi, Photoactive TiO<sub>2</sub>-montmorillonite composite for degradation of organic dyes in water, *Journal of Photochemistry and Photobiology A*, 295, 2014, 57-63.
- [20] A.N. Ökte, D. Tuncel, A.H. Pekcan and T. Özden, Characteristics of iron-loaded TiO<sub>2</sub>-supported montmorillonite catalysts:β-Naphthol degradation under UV-A irradiation, *Journal of Chemical Technology and Biotechnology*, 89, 2014, 1155-1167.
- [21] A.N. Ökte and E. Sayınsöz, Characterization and Photocatalytic Activity of TiO<sub>2</sub> Supported Sepiolite Catalysts, *Separation and Purification Technology*, 62, 2008, 535-543.



- [22] K. Chojnacka, A. Chojnacki and H. Gorecka, Biosorption of Cr<sup>3+</sup>, Cd<sup>2+</sup> and Cu<sup>2+</sup> ions by blue-green algae *Spirulina* sp.: kinetics, equilibrium and the mechanism of the process, *Chemosphere*, 59, 2005, 75-84.
- [23] L. Zhi-Yong, G. Si-Yuan and L. Lin, Study on the process, thermodynamical isotherm and mechanism of Cr(III) uptake by *Spirulina platensis*, *Journal of Food Engineering*, 75, 2006, 129-136.
- [24] Y. Kitayama, T. Kodama, M. Abe, H. Shimotsuma and Y. Matsuda, Synthesis of titania pillared saponite in aqueous solution of acetic acid, *Journal of Porous Materials*, 5, 1998, 121-126.
- [25] T. Kaneko, M. Fuji, T. Kodama, Y. Kitayama, Synthesis of titania pillared mica in aqueous solution of acetic acid, *Journal of Porous Materials*, 8, 2001, 99-109.
- [26] A. Georgaka and N. Spanos, Study of the Cu(II) removal from aqueous solutions by adsorption on Titania, *Global NEST Journal*, 12, 2010, 239-247.
- [27] E.W. Rice, R.B. Baird, A.D. Eaton and L.S. Clesceri, *Standard Methods for The Examination of Water and Wastewater*. (Washington, D.C.: American Public Health Association, 1992, 18th ed., pp. 59)
- [28] Y.F. Chen, C.Y. Lee, M.Y. Yeng and H.T. Chiu, The effect of calcinations temperature on the crystallinity of TiO<sub>2</sub> nanopowders, *Journal of Crystal Growth*, 247, 2003, 363-370.
- [29] C. Theivarasu and S. Mylsamy, Equilibrium and kinetic adsorption studies of Rhodamine-B from aqueous solutions using cocoa (*Theobroma cacao*) shell as a new adsorbent, *International Journal of Engineering Science and Technology*, 2, 2010, 6284–6292.
- [30] K. Haraguchi, T. Takehisa and S. Fan, Effects of clay content on the properties of nanocomposite hydrogels composed of poly(N-isopropylacrylamide) and clay, *Macromolecules*, 35, 2002, 10162-10171.
- [31] K. Haraguchi and H. J. Li, Mechanical properties and structure of polymer-clay nanocomposite gels with high clay content, *Macromolecules*, 39, 2006, 1898-1905.
- [32] J. Zhang, X. Wang, L. Lu, D. Li and X. Yang, Preparation and performance of high-impact polystyrene (HIPS)/nano-TiO<sub>2</sub> nanocomposites, *Journal of Applied Polymer Science*, 87, 2003, 381-385.
- [33] H. Salehian, S. Ahmad and J. Jahromi, Effect of titanium dioxide nanoparticles on mechanical properties of vinyl ester-based nanocomposites, *Journal of Composite Materials*, 49, 2015, 2365-2373.

Emre Tekay. "Effective adsorption of Cr (VI) ions onto titanium dioxide immobilized high strength polyacrylamide hydrogels." *International Journal of Engineering Science Invention(IJESI)*, vol. 6, no. 9, 2017, pp. 60–68.